

Simulating spin dynamics with quantum computers

Jarrett L. Lancaster* and D. Brysen Allen

Department of Physics, High Point University, One University Parkway, High Point, NC 27268

(Dated: July 22, 2022)

IBM quantum computers are used to simulate the dynamics of small systems of interacting quantum spins. For time-independent systems with $N \leq 2$ spins, we construct circuits which compute the exact time evolution at arbitrary times and allow measurement of spin expectation values. Larger systems with spins require a the Lie-Trotter decomposition of the time evolution operator, and we investigate the case of $N = 3$ explicitly. Basic readout-error mitigation is introduced to improve the quality of results run on these noisy devices. The simulations provide an interesting experimental component to the standard treatment of quantum spin in an undergraduate quantum mechanics course.

I. INTRODUCTION

The field of quantum computation has experienced tremendous growth in recent years. Originally suggested as the only possible way to simulate quantum mechanical systems with many degrees of freedom,¹ quantum computing algorithms have also been shown to play a valuable role in an efficient factorization scheme² which has dramatic implications for modern cryptographic systems.³ Though such devices are still far from capable of solving these classic problems, noisy, intermediate-scale quantum (NISQ) devices⁴ are widely available from providers such as Rigetti,⁵ IonQ,⁶ and IBM,⁷ The question for the foreseeable future is: what kinds of problems are these NISQ devices capable of solving?

While many potential uses for NISQ-era hardware have been proposed,⁸ one under-appreciated use for these devices is as a learning tool for quantum mechanics. As it happens, quantum computers are ideally suited for probing small spin systems,⁹ such as those that would be explored in an undergraduate course on quantum mechanics. Recent papers in this journal have explored some basic problems future quantum computers can conceivably be used to solve,¹⁰ employing the Grover search algorithm on actual quantum hardware,¹¹ using quantum computers to measure spin correlations,⁹ and applying basic error mitigation to improve results on currently available hardware.¹² Given the free availability of 1-7 qubit devices from IBM, the simulation of spin systems provides an incredible opportunity to give students a no-cost experimental component which complements the fairly abstract theory that is standard treatment in such a course.

In this paper, we present several types of spin simulations involving the time evolution of arbitrarily prepared initial states. The Qiskit software development kit (SDK)¹³ is used to encode time evolution in quantum circuits, which are then run on the cloud-based IBM hardware. Time evolution of a single spin is simulated by mapping the spin to a qubit and applying a single unitary gate corresponding to the exact time evolution operator. Results for two-spin and three-spin systems with nontrivial interactions are also presented. The scheme for performing time evolution on two-spin systems is exact, but it requires a more complicated circuit. We are forced to use approximate methods when constructing time evolution for systems with three or more spins, and it is shown that errors and noise inherent to currently-available devices make accurate re-

sults quite difficult to obtain for even systems of three spins.

The remainder of this paper is organized as follows. Section II contains a brief review of relevant spin physics and the essential ingredients needed to simulate spin systems on IBM's quantum hardware. The exact dynamics of single spins evolving in a magnetic field is explored. Lie-Trotter decomposition, essential for simulating systems with more than two spins, is introduced in Sec. III in the simplified context of a single spin, where the convergence of the method and practical limitations in its implementation can be demonstrated most clearly. Dynamics in interacting systems of two and three spins are shown in Sec. IV, and the Lie-Trotter decomposition is shown to be essential to performing time evolution in the three-spin system. Finally, a brief discussion is included in Sec. V.

II. SINGLE SPINS

A single spin- $\frac{1}{2}$ degree of freedom is a two-level system whose quantum state can be expressed as a linear combination of basis kets $|\psi\rangle = \alpha|+\rangle + \beta|-\rangle$, where $|\pm\rangle$ are eigenstates of the operator \hat{S}^z , satisfying

$$\hat{S}^z |\pm\rangle = \pm \frac{\hbar}{2} |\pm\rangle. \quad (1)$$

We follow standard notation for labeling the eigenstates of \hat{S}^z (e.g., Ref. 14), but we caution the reader with experience in quantum information theory that these labels refer to eigenstates of \hat{S}^x in other references.¹⁵ The complex amplitudes are constrained by the unit normalization of the quantum state $\langle\psi|\psi\rangle = |\alpha|^2 + |\beta|^2 = 1$. As the global phase of $|\psi\rangle$ is unobservable, a common parameterization is given by $\alpha = \cos \frac{\theta}{2}$, $\beta = e^{i\phi} \sin \frac{\theta}{2}$. To aid in calculations, the basis states can be represented by $|+\rangle \doteq (1, 0)^T$ and $|-\rangle \doteq (0, 1)^T$ so that the state $|\psi\rangle$ can be represented by the two-component vector

$$|\psi\rangle \doteq \begin{pmatrix} \cos \frac{\theta}{2} \\ e^{i\phi} \sin \frac{\theta}{2} \end{pmatrix}. \quad (2)$$

By employing the explicit matrix representations of the spin operators,

$$\begin{aligned}\hat{S}^x &\doteq \frac{\hbar}{2} \begin{pmatrix} 0 & 1 \\ 1 & 0 \end{pmatrix}, & \hat{S}^y &\doteq \frac{\hbar}{2} \begin{pmatrix} 0 & -i \\ i & 0 \end{pmatrix}, \\ \hat{S}^z &\doteq \frac{\hbar}{2} \begin{pmatrix} 1 & 0 \\ 0 & -1 \end{pmatrix},\end{aligned}\quad (3)$$

one may compute the expectation values of the spin operators $\langle \hat{S}^\alpha \rangle \equiv \langle \psi | \hat{S}^\alpha | \psi \rangle$ for the state in Eq. (2),

$$\begin{aligned}\langle \hat{S}^x \rangle &= \frac{\hbar}{2} \sin \theta \cos \phi, \\ \langle \hat{S}^y \rangle &= \frac{\hbar}{2} \sin \theta \sin \phi, \\ \langle \hat{S}^z \rangle &= \frac{\hbar}{2} \cos \theta.\end{aligned}\quad (4)$$

Thus, the parameters θ and ϕ correspond to angular coordinates which map the possible states to points on a unit sphere—also known as the Bloch sphere. Time evolution can be generated by interaction of the spin with a magnetic field \mathbf{B} via the Hamiltonian

$$\hat{H} = -\mu \mathbf{B} \cdot \hat{\mathbf{S}}, \quad (5)$$

where the constant μ represents the magnetic moment which allows the spin to couple to an external field. The time-dependent state $|\psi(t)\rangle$ is obtained by solving the Schrödinger equation,

$$i\hbar \frac{d}{dt} |\psi(t)\rangle = \hat{H} |\psi(t)\rangle, \quad (6)$$

given some initial state $|\psi(0)\rangle$. The calculation of $|\psi(t)\rangle$ is typically performed by representing \hat{H} as a 2×2 matrix and extracting separate, coupled, first-order equations for the time-dependent amplitudes $\alpha(t)$ and $\beta(t)$, which can be solved using standard methods. With the aim of simulating such dynamics on a quantum computer, it is convenient to take a different approach. One may write the formal solution as

$$|\psi(t)\rangle = \exp\left[-\frac{i}{\hbar} \hat{H} t\right] |\psi(0)\rangle \equiv \hat{U}(t) |\psi(0)\rangle, \quad (7)$$

and calculating the time-evolution operator $\hat{U}(t)$ explicitly as a 2×2 matrix. As matrix exponentiation is not always covered in introductory quantum mechanics, let us consider the specific example $\mathbf{B} = B_0 \hat{x}$ in detail. The time-evolution operator can be written

$$\hat{U}(t) = \exp\left[\frac{i\omega_0 t}{2} \hat{\sigma}^x\right], \quad (8)$$

where $\omega_0 \equiv \mu B_0$. Using the property that $[\hat{\sigma}^x]^2 = \hat{I}$, one may expand the exponential as a Taylor series, group even and odd

terms separately to obtain,

$$\begin{aligned}\hat{U}(t) &= \hat{I} \left(1 - \frac{(\omega_0 t/2)^2}{2!} + \frac{(\omega_0 t/2)^4}{4!} + \dots\right) \\ &\quad + i\hat{\sigma}^x \left(\omega_0 t/2 - \frac{(\omega_0 t/2)^3}{3!} + \frac{(\omega_0 t/2)^5}{5!} + \dots\right) \\ &= \cos \frac{\omega_0 t}{2} \hat{I} + i \sin \frac{\omega_0 t}{2} \hat{\sigma}^x \\ &\doteq \begin{pmatrix} \cos \frac{\tau}{2} & i \sin \frac{\tau}{2} \\ i \sin \frac{\tau}{2} & \cos \frac{\tau}{2} \end{pmatrix},\end{aligned}\quad (9)$$

where $\tau \equiv \omega_0 t$. Here we have made use of the Taylor expansions for $\sin \frac{\tau}{2}$ and $\cos \frac{\tau}{2}$ to sum the infinite series explicitly. For the specific initial state $|\psi(0)\rangle = |+\rangle$, one can employ Eqs. (2)–(3) to obtain

$$\begin{aligned}\langle \hat{S}^x(t) \rangle &= 0 \\ \langle \hat{S}^y(t) \rangle &= \frac{\hbar}{2} \sin \omega_0 t \\ \langle \hat{S}^z(t) \rangle &= \frac{\hbar}{2} \cos \omega_0 t.\end{aligned}\quad (10)$$

Equations (10) are the types of theoretical predictions we wish to test on a quantum computer. In a quantum computer, the fundamental object is a qubit which can exist in a superposition of two basis states, typically labeled $|0\rangle$ and $|1\rangle$. This basis is commonly referred to as the ‘‘computational basis.’’ A quantum spin may be represented by a qubit with the mapping

$$\begin{aligned}|+\rangle &\rightarrow |0\rangle, \\ |-\rangle &\rightarrow |1\rangle,\end{aligned}\quad (11)$$

Universal quantum computers execute circuits which consist of series of gates that modify the states of the qubits. To extract information about the system, some measurement must be performed. Thus, the three basic stages in a quantum circuit appropriate for simulating the spin dynamics discussed above are (1) state initialization, (2) time evolution of the state, and (3) measurement of the spin components. IBM’s quantum hardware automatically initializes each qubit to the state $|0\rangle$. A general quantum state of the form in Eq. (2) can be generated by applying the following unitary operator,

$$\hat{U}_3(\theta, \phi, \lambda) \doteq \begin{pmatrix} \cos \frac{\theta}{2} & -e^{i\lambda} \sin \frac{\theta}{2} \\ e^{i\phi} \sin \frac{\theta}{2} & e^{i(\phi+\lambda)} \cos \frac{\theta}{2} \end{pmatrix}. \quad (12)$$

Users may access quantum hardware through the Python-based Qiskit SDK.¹³ The Qiskit textbook¹⁵ provides an excellent overview to the basics of using Qiskit to construct quantum circuits, so we only sketch the main steps in translating state preparation and time evolution into a series of quantum gates. The reader is referred to other excellent resources^{9,15,16} for additional background information. Sample Jupyter notebooks containing programs used in this work are included in the supplemental material.¹⁷

The \hat{U}_3 gate is available as a three-parameter gate in Qiskit, `u(theta, phi, lambda)`. The operator in Eq. (12) is actually

more general than we require, as λ can be set to any value. However, as this operation is available as a built-in quantum gate for use on the IBM quantum devices, it provides a convenient mechanism for generating a qubit in an arbitrary state $|\psi(0)\rangle = \hat{U}_3(\theta, \phi, 0)|0\rangle$. Time evolution is performed by not-

ing that our expression for the time evolution operator $\hat{U}(t)$ in Eq. (8) may also be written in terms of the $\hat{U}_3(\theta, \phi, \lambda)$ gate as $\hat{U} = \hat{U}_3\left(\tau, +\frac{\pi}{2}, -\frac{\pi}{2}\right)$.

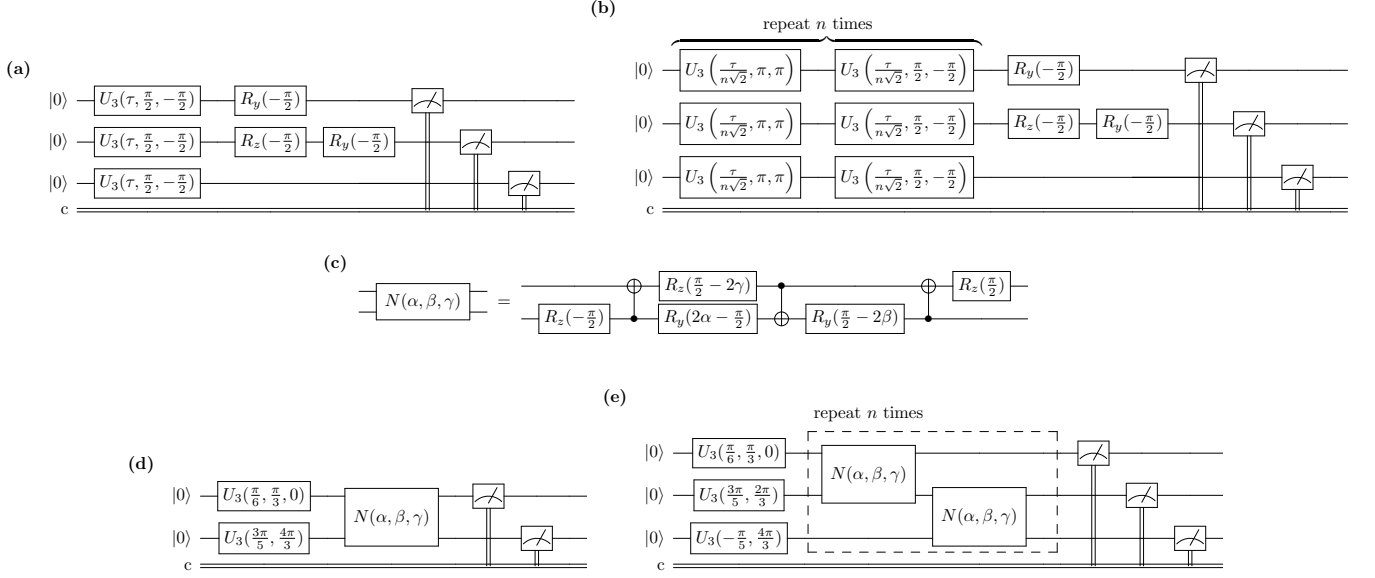


FIG. 1: Quantum circuits used to perform various tasks described in the main text; (a) circuit to perform time evolution and measure three spin components for a spin prepared in the state $|+\rangle$. As qubits are initialized into $|0\rangle$ by default, no additional state preparation stage is required, and the circuit consists only of time evolution provided by $\hat{U}_3\left(\tau, \frac{\pi}{2}, -\frac{\pi}{2}\right)$ followed by measurement. For the x - and y - components, state rotations are required before measuring in the computational basis, as discussed in the main text; (b) circuit to perform time evolution and measure three spin components; (c) circuit for exact exponentiation of $\exp[i\alpha\hat{\sigma}^x \otimes \hat{\sigma}^x + i\beta\hat{\sigma}^y \otimes \hat{\sigma}^y + i\gamma\hat{\sigma}^z \otimes \hat{\sigma}^z]$; (d) circuit for exact time evolution of the two-spin state in Eq. (26) with Hamiltonian in Eq. (23) for $J_x = 0.5J$, $J_y = -0.45J$, $J_z = 0.25J$; (e) circuit for approximate time evolution of a three-spin state with Hamiltonian in Eq. (31) for $J_x = 0.5J$, $J_y = -0.45J$, $J_z = 0.25J$.

When using IBM quantum devices, it is only possible to make a direct measurement in the computational basis. That is, for a qubit in the state $|\psi\rangle = \alpha|0\rangle + \beta|1\rangle$, a measurement will only return 0 or 1 corresponding to the states $|0\rangle$ or $|1\rangle$, respectively. This constraint suggests one is only able to measure \hat{S}^z directly in a spin dynamics simulation. Reference 9 notes that one can measure spin along any axis (or equivalently, the qubit in any basis) by an appropriate rotation of the system before performing the measurement in the computational basis. Within Qiskit, one may directly apply rotation gates (e.g., $\mathbf{R}_x(\theta)$ for a rotation of angle θ about the x -axis) to the quantum state. To measure spin about the x -axis, one first performs rotations on the system which bring the vector $\hat{\mathbf{x}}$ into alignment with the z -axis. Explicitly, $\hat{\mathbf{z}} = \mathbf{R}_y\left(-\frac{\pi}{2}\right)\hat{\mathbf{x}} = \mathbf{R}_y\left(-\frac{\pi}{2}\right)\mathbf{R}_z\left(-\frac{\pi}{2}\right)\hat{\mathbf{y}}$. This rotation process is depicted pictorially in Fig. 2 for some arbitrary axis, $\hat{\mathbf{n}}$.

As IBM quantum devices are available for use by anyone

in the world, jobs are often queued—sometimes for significant times. With efficiency in mind, it is convenient embed three independent, single-spin circuits into a single three-qubit circuit to measure all three spin components in a single job. The circuit shown in Fig. 1a creates three copies of this single spin, performs identical time evolution on each spin, and then measures one of the three spin components on each qubit. Using Qiskit, the circuit in Fig. 1a can be constructed and sent to IBM quantum devices for execution.

When one executes the quantum circuit in Fig. 1a, the result yields a sequence of three digits, each being either 0 or 1, which is written to the “classical register.” For example, one might obtain the readout ‘100’, indicating that $+\frac{\hbar}{2}$ was obtained for \hat{S}^x and \hat{S}^y , while $-\frac{\hbar}{2}$ was obtained for \hat{S}^z .¹⁸ The framework of quantum mechanics does not allow for meaningful predictions about the outcome of a single such experiment. Instead, we are limited in being able to compute statistical quantities such as probabilities and expectation values,

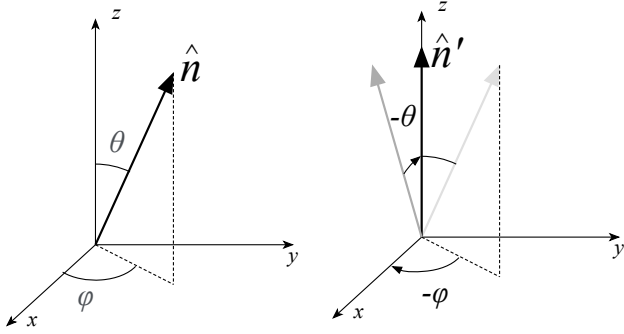


FIG. 2: To measure spin about the axis $\hat{\mathbf{n}}$, one must perform the required rotations to bring $\hat{\mathbf{n}}$ into alignment with the z -axis (the computational basis). Given polar-spherical angles θ, ϕ corresponding to $\hat{\mathbf{n}}$, one finds $\hat{\mathbf{n}}' \equiv \hat{\mathbf{z}} = \mathbf{R}_y(-\theta) \mathbf{R}_z(-\phi) \hat{\mathbf{n}}$.

which give us information about the averages of many repetitions of an experiment performed on identically prepared systems. Typically, one executes a circuit for some large number of “shots,” $N_{\text{shots}} \gg 1$, so that experimental averages can be constructed for comparison to the theoretical predictions (e.g., Eqs. 10). In Qiskit, the counts associated with executing a circuit over some number of shots is returned a Python dictionary of the form ‘state’ : counts. Here ‘state’ is a string corresponding to a possible three-qubit state (e.g., ‘010’ \rightarrow $|010\rangle$) and counts is the number of shots for which this state was written to the classical register. From this information, we construct spin expectation values as follows. Let n_{abc} be the counts for state $|abc\rangle$, where $a, b, c \in \{0, 1\}$. Taking $\langle \hat{S}^y \rangle$ as an example, we have eight counts, $n_{000}, n_{001}, \dots, n_{111}$. A weighted average of this spin component is given by

$$\langle \hat{S}^y \rangle = \frac{1}{N_{\text{shots}}} \left[(n_{000} + n_{001} + n_{100} + n_{101}) \left(+\frac{\hbar}{2} \right) + (n_{010} + n_{011} + n_{110} + n_{111}) \left(-\frac{\hbar}{2} \right) \right] \quad (13)$$

Note that the counts for which the middle qubit is measured to be $|0\rangle$ (corresponding to spin “up”) weight the contribution of $+\frac{\hbar}{2}$, while those in which the middle qubit is in $|1\rangle$ (corresponding to spin “down”) weight the contribution of $-\frac{\hbar}{2}$. Analogous averaging can be performed on the other qubits to obtain experimental values for the expected averages $\langle \hat{S}^x \rangle, \langle \hat{S}^z \rangle$. Results from running the circuit in Fig. 1a on *ibmq_casablanca* (v 1.2.35, a Falcon r4H processor) with $N_{\text{shots}} = 8192$ are shown in Fig. 3. Error bars shown are statistical estimates given by $\sigma/\hbar \approx \frac{1}{2\sqrt{N_{\text{shots}}}}$.

The framework outlined in this section allows one to simulate the dynamics of a single spin in an external magnetic field. Straightforward generalizations for students could consist of applying an additional \hat{U}_3 gate before time evolution to create an arbitrary initial state or applying additional rotations before measurement to measure spin about a specified axis. Additionally, one could investigate a magnetic field pointing along a different direction. For example, consider the magnetic field $\mathbf{B} = \frac{B_0}{\sqrt{2}} (\hat{\mathbf{x}} + \hat{\mathbf{y}})$. One can repeat the basic steps leading to

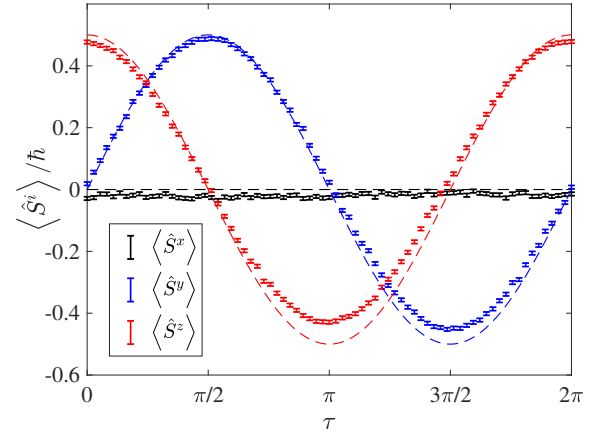


FIG. 3: Theory (dashed lines) and actual results (markers with error bars) for time evolution of spin components with $\mathbf{B} = B_0 \hat{\mathbf{x}}$ and $|\psi(0)\rangle = |+\rangle$ using circuit shown in Fig. 1a on *ibmq_casablanca* (v 1.2.35, a Falcon r4H processor).

Eq. (9) to obtain

$$\exp \left[i \frac{\omega_0 t}{2\sqrt{2}} (\hat{\sigma}^x + \hat{\sigma}^y) t \right] = \hat{U}_3 \left(\tau, \frac{3\pi}{4}, -\frac{3\pi}{4} \right). \quad (14)$$

To simulate the dynamics generated by this new magnetic field, one only needs to replace $\hat{U}_3 \left(\tau, \frac{\pi}{2}, -\frac{\pi}{2} \right)$ in the circuit in Fig. 1a by $\hat{U} \left(\tau, \frac{3\pi}{4}, -\frac{3\pi}{4} \right)$. The experimental and theoretical results for this system are shown in Fig. 4. Theoretical spin expectation values are obtained from direct exponentiation of the left side of Eq. (14) to compute $|\psi(t)\rangle$ in Eq. (7). Time-dependent expectation values of the spin operators in Eqs. (3) give

$$\begin{aligned} \langle \hat{S}^x(t) \rangle &= -\frac{\hbar}{2\sqrt{2}} \sin \omega_0 t, \\ \langle \hat{S}^y(t) \rangle &= \frac{\hbar}{2\sqrt{2}} \sin \omega_0 t, \\ \langle \hat{S}^z(t) \rangle &= \frac{\hbar}{2} \cos \omega_0 t. \end{aligned} \quad (15)$$

Note that despite using a circuit with three qubits, the individual qubits are uncoupled and do not interact. The circuit in Fig. 1a represents three copies of a single qubit circuit, with the individual qubits only experiencing different rotations prior to measurement so that all three spin expectation values can be computed within a single job. In the next sections, we develop the machinery required to explore time evolution in multispin systems in which the spins interact. This added complexity will necessitate the introduction of multiple-qubit gates. Before turning attention to the interaction of multiple spins, we first introduce a technique for simulating dynamics in more complex Hamiltonians: the Lie-Trotter decomposition.

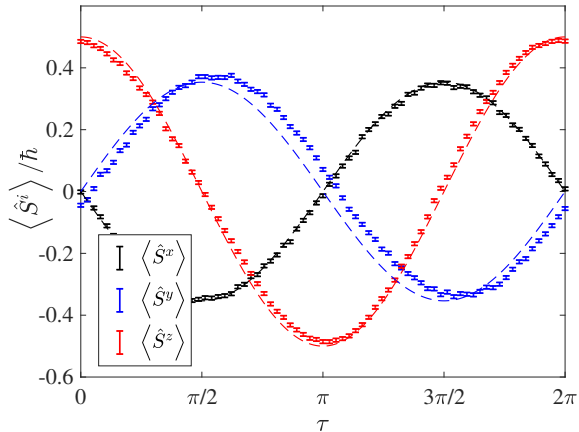


FIG. 4: Theory/results for time evolution of spin components using `ibmq_lagos` (v 1.0.06, a Falcon r5.11H processor) with $\mathbf{B} = \frac{B_0}{\sqrt{2}}(\hat{x} + \hat{y})$ and $|\psi(0)\rangle = |+\rangle$.

III. LIE-TROTTER DECOMPOSITION

For arbitrary systems, it is not possible to compute the exact time evolution operator $\hat{U}(t)$ in general. In this work, we only consider time-independent interactions. While certain classes of these models can be solved exactly,¹⁹ it is generally necessary to use approximate techniques for interacting systems. One such approximation scheme for computing the time evolution operator relies on splitting the Hamiltonian into non-commuting pieces for which time evolution of each subsystem can be computed exactly. By computing the corresponding parts of the time evolution separately and layering the action of these operators over a large number of substeps, the approximate time evolution will converge to the exact result as the number of substeps approaches infinity. This technique is known as a Lie-Trotter decomposition,²⁰ and below we introduce the method using a particularly simple system.

Consider a Hamiltonian which is composed of two parts which do not commute.

$$\hat{H} = \hat{A} + \hat{B}, \quad (16)$$

with $[\hat{A}, \hat{B}] \neq 0$. As a simple example, let us take the single spin in a magnetic field with $\mathbf{B} = \frac{B_0}{\sqrt{2}}(\hat{x} + \hat{y})$ considered in the previous section so that

$$\hat{H} = \frac{\omega_0}{\sqrt{2}}[\hat{\sigma}^x + \hat{\sigma}^y]. \quad (17)$$

In this case, $\hat{A} = \frac{\omega_0}{\sqrt{2}}\hat{\sigma}^x$ and $\hat{B} = \frac{\omega_0}{\sqrt{2}}\hat{\sigma}^y$, and the commutator

of these pieces is demonstrably nonzero,

$$[\hat{A}, \hat{B}] = \frac{\omega_0^2}{2}[\hat{\sigma}^x, \hat{\sigma}^y] = i\frac{\omega_0^2}{2}\hat{\sigma}^z \neq 0. \quad (18)$$

The time-evolution operator for this system is given by

$$\hat{U}(t) = \exp[-i\hat{H}t/\hbar] = \exp[-i\hat{A}t/\hbar - i\hat{B}t/\hbar]. \quad (19)$$

In Sec. II, we computed $\hat{U}(t)$ exactly. In general, such exact computations are not possible, so here we take an alternative approach. Let us define the operators

$$\hat{U}_A(t) = \exp[-i\hat{A}t/\hbar], \quad \hat{U}_B(t) = \exp[-i\hat{B}t/\hbar]. \quad (20)$$

As \hat{A} and \hat{B} do not commute, $\hat{U}(t) \neq \hat{U}_A(t)\hat{U}_B(t)$. However, according to the Lie-Trotter product formula,²⁰ we can say

$$\begin{aligned} & \exp[i(\hat{A} + \hat{B})t/\hbar] \\ &= \lim_{n \rightarrow \infty} \left(\exp[-i\hat{A}t/n\hbar] \exp[-i\hat{B}t/n\hbar] \right)^n, \end{aligned} \quad (21)$$

or

$$\hat{U}(t) = \lim_{n \rightarrow \infty} \left(\hat{U}_A\left(\frac{t}{n}\right) \hat{U}_B\left(\frac{t}{n}\right) \right)^n. \quad (22)$$

That is, if we subdivide a time step into n sub-steps, the product of exponentials will converge to the true expression for $\hat{U}(t)$ as $n \rightarrow \infty$. The particular example of the magnetic field in the xy -plane is instructive, as the exact solution for $\hat{U}(t)$ is available for comparison. For the single-spin Hamiltonian in Eq. (17), a circuit based on the Trotter decomposition in Eq. (22) is shown in Fig. 1b. Results from running this circuit on the QASM simulator are shown in Fig. 5a for several choices of n . The QASM simulator uses classical computation to simulate results for a given quantum circuit on a noiseless device, clearly demonstrating the convergence of the Trotter decomposition on “ideal” hardware. We note that including more Trotter steps requires more circuit gates, leading to an increased circuit *depth*. In actual hardware, larger circuit depth is correlated with a larger accumulation of errors. While more steps lead to better Trotter convergence, adding more steps also increases errors. Results for different choices of n obtained from actual quantum hardware (`ibmq_manila`, v1.0.10, a Falcon r5.11L processor) are shown in Fig. 5b and depict the initial convergence is eventually washed out by the accumulation of errors as n increases. A choice of $n \sim 10$ appears to be the best for balancing errors due to circuit depth and errors due to finite Trotter steps in this simple circuit on this particular device.

Of course, the time evolution operator corresponding to the

Hamiltonian in Eq. (5) with $\mathbf{B} = \frac{B_0}{\sqrt{2}}(\hat{x} + \hat{y})$ has been given

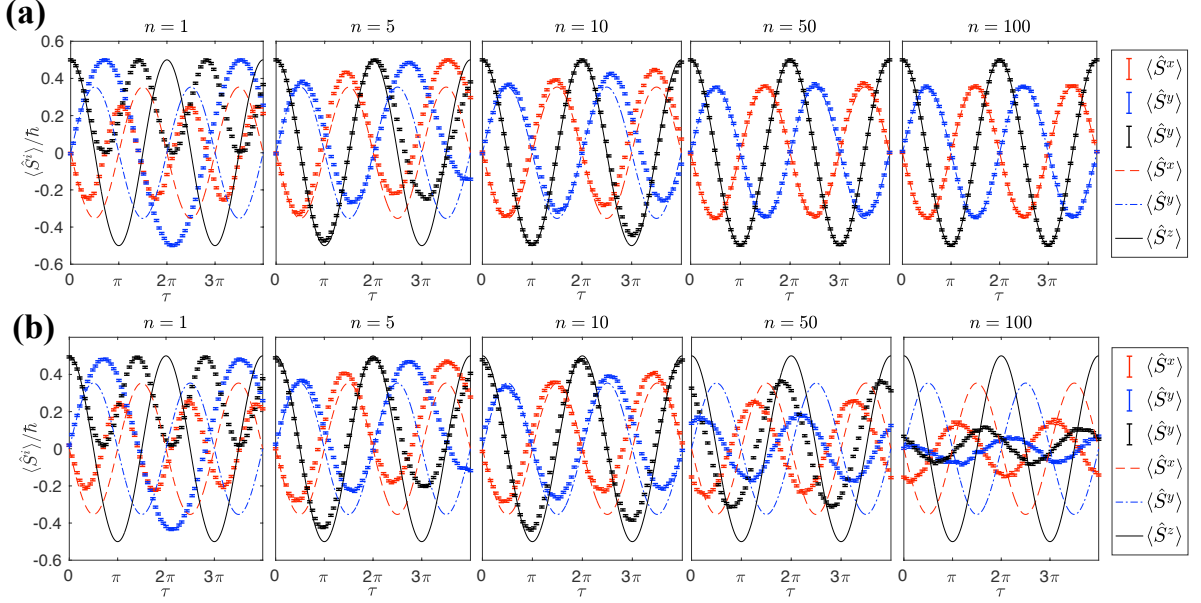


FIG. 5: (a) Theory/simulated (QASM simulator) results for time-dependent spin components with $\mathbf{B} = \frac{B_0}{\sqrt{2}} (\hat{x} + \hat{y})$ and $|\psi(0)\rangle = |+\rangle$ with variable number of Trotter steps; (b) theory/results for $\mathbf{B} = \frac{B_0}{\sqrt{2}} (\hat{x} + \hat{y})$ and $|\psi(0)\rangle = |+\rangle$ with variable number of Trotter steps using `ibmq_manila v1.0.10`, a Falcon r5.11L processor.

exactly in Eq. (14). For even modestly more complicated systems, it is generally not possible to obtain an exact form for the time evolution operator, so a similar Trotter decomposition will be essential to simulating the dynamics. The aims of this section have been to illustrate the algorithm in a simple setting while also highlighting the accumulation of errors associated with increasing circuit depth. Accurate simulation of interesting systems on actual quantum hardware is a challenging endeavor as adding Trotter steps aids in the convergence of the algorithm while also contributing costly errors to the calculation. Reasonable accuracy has been obtained²¹ for systems of $n \sim 10$ spins using no more than $n = 5$ steps for short times. We note that our computations use exactly n Trotter steps for each time step for conceptual simplicity. In certain applications, it might be desirable to use a variable number of Trotter steps so that circuit depth can be decreased at shorter times.

In the next section, we will explore small systems of interacting spins and demonstrate how Trotter decomposition may be used to simulate dynamics. As a first step, we will show how the case of $N = 2$ spins can be simulated exactly, paving the way for using the Lie-Trotter decomposition to investigate larger systems.

IV. MULTIPLE SPINS

A. $N = 2$

With the ability to decompose the time evolution operator approximately into a product of simpler factors, we now turn attention to the problem of multiple spins which interact. For

the simplest case, $N = 2$, a fairly general interaction Hamiltonian is given by

$$\hat{H} = -J_x \hat{S}^x \otimes \hat{S}^x - J_y \hat{S}^y \otimes \hat{S}^y - J_z \hat{S}^z \otimes \hat{S}^z, \quad (23)$$

where the $J_{x,y,z}$ are couplings. Semi-classically, Eq. (23) is motivated by the classical result that the energy contained in the electromagnetic field of two magnetic dipoles $\vec{\mu}_{1,2}$ is proportional to $-\vec{\mu}_1 \cdot \vec{\mu}_2$ so that aligned spins are energetically favorable. We will proceed with couplings as arbitrarily tunable parameters to explore how to simulate such a system on a quantum computer. To this end, the basic task is to compute the time evolution operator $U(t) = \exp[-i\hat{H}t]$. For brevity, we employ units in which $\hbar \rightarrow 1$ for the remainder of this paper. The circuit shown in Fig. 1c depicts a representation of the two-qubit operation $\exp[-\alpha\hat{\sigma}^x \otimes \hat{\sigma}^x - \beta\hat{\sigma}^y \otimes \hat{\sigma}^y - \gamma\hat{\sigma}^z \otimes \hat{\sigma}^z]$. The two-qubit gates are known as “controlled NOT” (CNOT) gates, which perform the following operation

$$|0\rangle \rightarrow |1\rangle, \quad |1\rangle \rightarrow |0\rangle, \quad (24)$$

on the “target” qubit *only* if the “control” qubit is in the state $|1\rangle$. In the circuit diagram, the target qubit is denoted by the “+” and connected to the control qubit. Employing the Qiskit convention for state labels, the action of this gate on two qubit states can be summarized as

$$\begin{aligned} \text{CNOT}|00\rangle &= |00\rangle, & \text{CNOT}|01\rangle &= |11\rangle, \\ \text{CNOT}|10\rangle &= |10\rangle, & \text{CNOT}|11\rangle &= |01\rangle, \end{aligned} \quad (25)$$

with the qubits arranged in the form $|\text{target}, \text{control}\rangle$. Two-qubit gates such as CNOT typically lead to errors which are

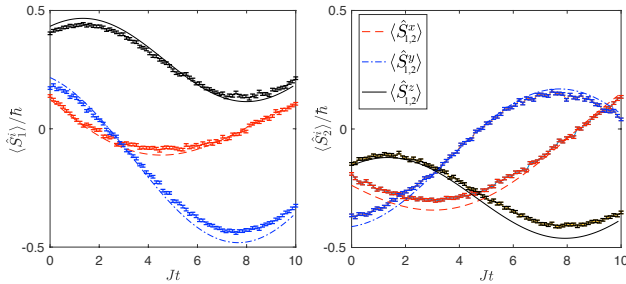


FIG. 6: Time-dependence of spin expectation values for an interacting, two-spin system using `ibmq_bogota` to simulate the model in Eq. (23) with the initial state given by Eq. (26).

an order of magnitude larger than those associated with single-qubit gates.²¹ Thus it is desirable to use a minimum number of CNOT gates. The circuit in Fig. 1c actually shows an optimal representation of the corresponding operator, using only three CNOT gates.^{21–23} Setting $\alpha = -J_x/4$, $\beta = -J_y/4$ and $\gamma = -J_z/4$, the exact time evolution operator $\hat{U}(t)$ corresponding to Eq. (23) is given by $N(\alpha, \beta, \gamma)$.

As a specific example, let us take $J_x = 0.5J$, $J_y = -0.45J$, $J_z = 0.25J$ for some arbitrary energy scale J and simulate time evolution on an actual quantum computer. We take the following initial single-qubit states

$$\begin{aligned} |\psi_1\rangle &= \cos\frac{\pi}{12}|+\rangle + e^{i\frac{\pi}{3}}\sin\frac{\pi}{12}|-\rangle, \\ |\psi_2\rangle &= \cos\frac{3\pi}{10}|+\rangle + e^{i\frac{4\pi}{3}}\sin\frac{3\pi}{10}|-\rangle. \end{aligned} \quad (26)$$

and plot as a function of dimensionless time Jt . The initial state chosen is $|\psi(0)\rangle = |\psi_1(0)\rangle \otimes |\psi_2(0)\rangle$. This system is simulated with the circuit shown in Fig. 1d with results collected from the device `ibmq_bogota v1.4.50`, a Falcon r4L processor. The theoretical predictions are obtained by calculating $|\psi(t)\rangle = e^{-i\hat{H}t/\hbar}|\psi(0)\rangle$ via an explicit exponentiation of the Hamiltonian matrix with the function `expm()` in `MATLAB`.²⁴ A script which computes the theoretical predictions is included in the supplemental material.¹⁷

B. $N > 2$

In this last subsection, we sketch how to obtain results for larger systems. For $N \geq 3$, it is generally not possible to perform exact time evolution. An exact representation of the time evolution in terms of quantum gates is generally only possible for models which can be diagonalized analytically and are “exactly solvable.” Though such models do exist¹⁹, the aim of this section is to equip the reader with tactics for the more general situation. The basic strategy for models with only nearest-neighbor interactions is to write the Hamiltonian as a sum of two-spin operators and use a Lie-Trotter decomposition to represent the time-evolution operator approximately as a product of two-spin time evolution operators. Consider a Hamiltonian \hat{H} of the form

$$\hat{H} = \sum_{i,j} \hat{h}_{ij}, \quad (27)$$

where \hat{h}_{ij} represents a direct interaction between qubits i and j . Most IBM devices allow for the application of CNOT gates between small subsets of nearest-neighbor qubits. Applying CNOT gates to qubits which are not directly connected is possible through the application of a series of so-called SWAP gates.¹⁵ In the interest of minimizing circuit depth, we only consider nearest-neighbor interactions in small systems which can be mapped to physically-connected qubits. To apply the Trotter decomposition to the time-evolution operator, one writes

$$\hat{U}(t) = \exp\left[-it \sum_{i,j} \hat{h}_{ij}\right] \approx \prod_{n=1}^n \prod_{i,j} e^{-i(t/n)\hat{h}_{ij}}. \quad (28)$$

Each factor of $e^{-i(t/n)\hat{h}_{ij}}$ corresponds to the circuit gate $\hat{N}(\alpha, \beta, \gamma)$ shown in Fig. 1c, which contains three CNOT gates. One would like the number of Trotter steps n as large as possible for the Trotter expansion to converge. But as the CNOT gates are the most largely responsible for errors in the results, it is desirable to use as few as possible. The current state-of-the-art for time evolution of many-spin systems is thus constrained by some optimal choice of n which maximizes convergence while minimizing errors from CNOT gates. It has been shown²¹ that this optimization results in extremely limited timescales for accurate computation for systems $n \sim \mathcal{O}(10)$.

With errors affecting the results so significantly, one can legitimately wonder about the value in today’s NISQ hardware. One approach to squeezing as much power as possible out of today’s devices is to implement some type of *error correction scheme* to the bare results.¹² A particularly simple scheme involves correcting counts for possible readout errors based on a short calibration experiment.¹⁵ Consider a simple circuit which creates the state $|001\rangle$ and then measures the state of each qubit. It is likely that most counts will return the correct state, but due to noise and measurement error, there will be instances of other states (e.g., $|000\rangle$, $|011\rangle$, etc.). Converting the counts into probabilities ($p_j = n_j/N_{\text{shots}}$), we collect these probabilities as a row vector. Repeating this process for all possible three qubit-states and collecting these rows yields an 8×8 *calibration matrix* \mathbf{C} . The matrix multiplication $\mathbf{C}(N, 0, 0, \dots, 0)^T$ then gives the actual counts obtained when the state $|000\rangle$ is created. For a circuit that simply creates and measures a given state, it is plausible that a significant source of error is the readout process. We can interpret these probabilities as average probabilities for various readout errors and apply the calibration to results for *any* circuit. If $\mathbf{x}_{\text{ideal}}$ are the ideal counts that would be obtained in the absence of readout errors and $\mathbf{x}_{\text{actual}}$ are the actual counts, the relationship is

$$\mathbf{x}_{\text{actual}} = \mathbf{C}\mathbf{x}_{\text{ideal}}. \quad (29)$$

Running a job returns counts contained in $\mathbf{x}_{\text{actual}}$, but one is interested in the ideal results, which can be obtained from the actual results by inverting the calibration matrix,

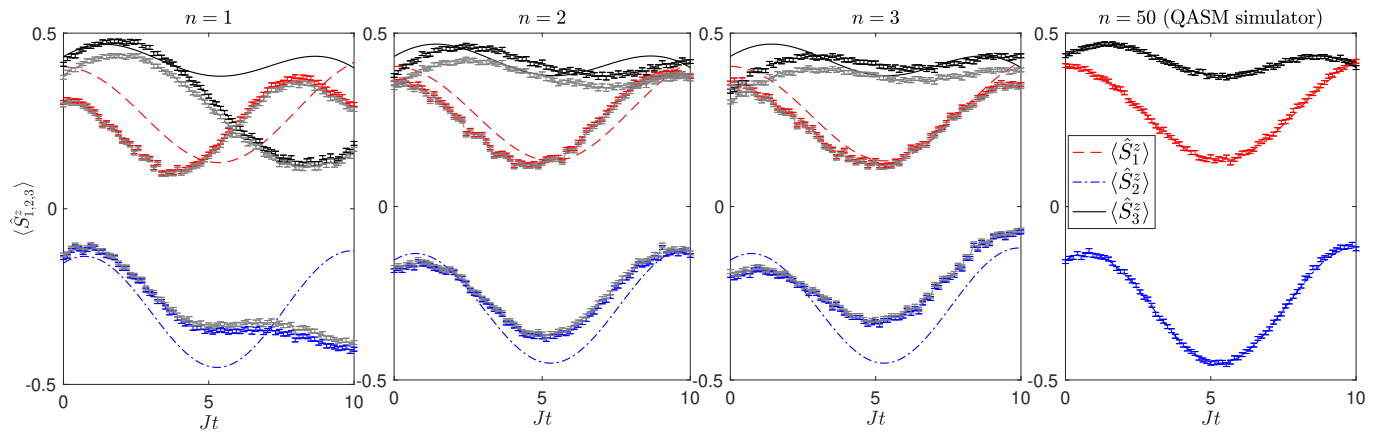


FIG. 7: Approximate time evolution of spin expectation values for variable number of Trotter steps using `ibm_perth` to simulate the model in Eq. (31) with initial state given in the main text. Rudimentary measurement error mitigation as described in the main text is applied to the results in the first three panels. Uncorrected results are depicted faintly alongside the main results. The right-most panel ($n = 50$) is obtained from the QASM simulator.

$$\mathbf{x}_{\text{ideal}} = \mathbf{C}^{-1} \mathbf{x}_{\text{actual}}. \quad (30)$$

Some caveats should be mentioned regarding the application of Eq. (30). For a low-noise device, one expects \mathbf{C} to be “close” to the identity matrix in that the diagonal entry is the largest (significantly so) of each row. There is no guarantee that \mathbf{C} is invertible, so one commonly uses a pseudoinverse matrix for such cases. Generally, a strict multiplication will result in non-integer values for the corrected counts. One could round to integer values, but the non-integer values cause no observable problems when used in the computation of expectation values, especially for a large number of shots. We employ this simplest version of error correction in results discussed below.

We consider three spins, each initialized to the state given in Eq. (2) with $\theta_1 = \frac{\pi}{6}$, $\phi_1 = \frac{\pi}{3}$, $\theta_2 = \frac{3\pi}{5}$, $\phi_2 = \frac{4\pi}{3}$, $\theta_3 = -\frac{\pi}{5}$, $\phi_3 = \frac{2\pi}{3}$. An “open” chain with interactions between nearest neighbors is used with

$$\begin{aligned} \hat{H} = & -J_x [\hat{S}^x \otimes \hat{S}^x \otimes \hat{I} + \hat{I} \otimes \hat{S}^x \otimes \hat{S}^x] \\ & - J_y [\hat{S}^y \otimes \hat{S}^y \otimes \hat{I} + \hat{I} \otimes \hat{S}^y \otimes \hat{S}^y] \\ & - J_z [\hat{S}^z \otimes \hat{S}^z \otimes \hat{I} + \hat{I} \otimes \hat{S}^z \otimes \hat{S}^z] \end{aligned} \quad (31)$$

V. DISCUSSION

We have presented schemes for simulating small ($N \leq 3$) spin systems on IBM quantum computers and measuring the time-dependent expectation values of various spin components. Systems of size $N = 1, 2$ have been treated exactly, and the results were subject to modest errors due to the compact circuits used. For larger systems, approximate schemes

A schematic circuit for performing approximate time evolution for $\langle \hat{S}_j^z(t) \rangle$ is shown in Fig. 1e. The error-mitigated results from `ibm_perth` v1.1.14, a Falcon r5.11H processor, are depicted alongside theoretical predictions in Fig. 7 for $n = 1, 2, 3$ Trotter steps. The challenge of simulating even a three-spin system is evident from the observation that $n = 2$ yields notably better agreement between experiment and theory than $n = 1$, but significant degradation occurs upon increasing the number of Trotter steps to $n = 3$. The noiseless QASM simulator is unaffected by CNOT errors, as shown by the excellent agreement between simulation and experiment when the number of Trotter steps is increased significantly to $n = 50$. We note that the theoretical prediction is obtained from exact diagonalization without Trotter decomposition, so the right-most panel in Fig. 7 demonstrates that the Trotter decomposition itself indeed converges to the exact result for a sufficiently large number of Trotter steps.

must be employed to perform time evolution. A Lie-Trotter decomposition was used to approximate the time evolution operator in a three-spin system. Even in a system with as few as three spins, the tradeoff between adding circuit elements to yield convergence of the algorithm and reducing circuit elements to minimize noise becomes apparent.

The dynamics of small spin systems are treated frequently in introductory quantum mechanics. The use of free, cloud-

based IBM hardware provides a highly accessible opportunity for students to explore these systems experimentally. In order to compare experimental results with theoretical predictions, students gain valuable experience in extracting experimental values of physical observables by manipulating the raw counts which are returned from the quantum circuit executions. Students must wrestle with what it means to “measure” a quantum mechanical observable, averaging a large number of independent results and computing statistical uncertainties. Extensions of the problems presented could form the basis of student projects in which the basic tools are applied to more complex systems (e.g., larger systems using the QASM simulator, time-dependent systems, etc.).

In addition to providing a useful and accessible experimental component to the traditional undergraduate treatment of quantum mechanics, these types of simulations give students experience with cutting-edge technology. In this sense, the seemingly-abstract content in a quantum mechanics course has direct relevance to a field in industry in which massive resources are being committed by IBM and other organizations. Excellent resources²⁵ are being developed for intro-

ducing quantum computing to students without a strong background in physics. We hope the present work is a useful demonstration of how quantum hardware can be used to explore physics that also shows how some familiarity with quantum mechanics can be leveraged to gain expertise using this emerging technology.

Acknowledgments

The authors acknowledge the use of IBM Quantum services for this work. The views expressed are those of the authors, and do not reflect the official policy or position of IBM or the IBM Quantum team. Additionally, the authors acknowledge the access to advanced services provided by the IBM Quantum Researchers Program.²⁶

* Electronic mail: jllancas2@highpoint.edu

- ¹ R. P. Feynman, “Simulating physics with computers,” *Int. J. Theor. Phys.* **21**, 467–488 (1982).
- ² P. W. Shor, “Polynomial-Time Algorithms for Prime Factorization and Discrete Logarithms on a Quantum Computer,” *SIAM J. Comput.* **26**(5), 1484–1509 (1997).
- ³ R. L. Rivest, A. Shamir, and L. Adleman, “A Method for Obtaining Digital Signatures and Public-Key Cryptosystems,” *Commun. ACM* **21**(2) 120–126 (1978).
- ⁴ J. Preskill, “Quantum Computing in the NISQ era and beyond,” *Quantum* **2**, 79 (2018).
- ⁵ Rigetti: <https://www.rigetti.com/>
- ⁶ IonQ: <https://ionq.com/>
- ⁷ IBM Quantum: <https://quantum-computing.ibm.com/>
- ⁸ Y. Alexeev, D. Bacon, K. R. Brown, R. Calderbank, L. D. Carr, F. T. Chong, B. DeMarco, D. Englund, E. Farhi, B. Fefferman, A. V. Gorshkov, A. Houck, J. Kim, S. Kimmel, M. Lange, S. Lloyd, M. D. Lukin, D. Maslov, P. Maunz, C. Monroe, J. Preskill, M. Roetteler, M. J. Savage, and J. Thompson, “Quantum Computer Systems for Scientific Discovery,” *PRX Quantum* **2**(1), 017001 (2021).
- ⁹ J. Brody and G. Guzman, “Calculating spin correlations with a quantum computer,” *Am. J. Phys.* **89**(1), 35–40 (2021).
- ¹⁰ D. Candela, “Undergraduate computational physics projects on quantum computing,” *Am. J. Phys.* **83**(8), 688–702 (2015).
- ¹¹ B. Kain, “Searching a quantum database with Grover’s search algorithm,” *Am. J. Phys.* **89**(6), 618–626 (2021).
- ¹² S. Johnstun and J-F. Van Huele, “Understanding and compensating for noise on IBM quantum computers,” *Am. J. Phys.* **89**(10), 935–942 (2021).
- ¹³ Qiskit: <https://qiskit.org>
- ¹⁴ D. H. McIntyre, C. A. Manogue, and J. Tate, *Quantum Mechanics*, (Pearson, New York, 2012).
- ¹⁵ A. Abbas, S. Andersson, A. Asfaw, A. Corcoles, L. Bello, Y. Ben-Haim, *et al.*, *Learn Quantum Computation Using Qiskit*, <https://community.qiskit.org/textbook>, (2020).
- ¹⁶ M. A. Nielsen and I. L. Chuang, *Quantum Computation and Quantum Information*, (Cambridge University Press, Cambridge, 2010).
- ¹⁷ Supplemental material available at <https://github.com/jllancas/SimulatingSpinsQComp>
- ¹⁸ IBM uses a qubit naming convention which is opposite to the convention used for labeling many-particle states in physics. For example, in the state $|\psi\rangle = |100\rangle$ the *bottom* qubit in the circuit diagram is in the state $|1\rangle$ rather than the top qubit.
- ¹⁹ A. Cervera-Lierta, “Exact Ising model simulation on a quantum computer,” *Quantum* **2**, 114 (2018).
- ²⁰ H. F. Trotter, “On the product of semi-groups of operators,” *Proc. Am. Math. Soc.* **10**(4), 545–551 (1959).
- ²¹ A. Smith, M. S. Kim, F. Pollmann, and J. Knolle, “Simulating quantum many-body dynamics on a current digital quantum computer,” *npj Quantum Information* **5**, 106 (2019).
- ²² F. Verstraete, J. I. Cirac, and J. I. Latorre, “Quantum circuits for strongly correlated quantum systems,” *Phys. Rev. A* **79**, 032316 (2009).
- ²³ A CNOT (controlled-NOT) gate is a two-qubit gate which applies the logical NOT operation to a target qubit *if* the control qubit is measured to be in the state $|1\rangle$, leaving the target qubit unchanged otherwise. Two-qubit gates are essential for simulating systems in which qubits *interact*. The reader is encouraged to consult Ref. 15 for detailed information about CNOT gates and their use in Qiskit.
- ²⁴ MATLAB. version 9.10.0.1669831 (R2021a Update 2). Natick, Massachusetts: The MathWorks Inc.; 2021.
- ²⁵ C. Hughes, J. Isaacson, A. Perry, R. F. Sun, and J. Turner, *Quantum Computing for the Quantum Curious*, (Springer, Berlin, 2021).
- ²⁶ IBM Quantum Researchers Program: <https://quantum-computing.ibm.com/programs/researchers>